

CHANGE IN OPERATING PARAMETERS OF TURBOCHARGED DIRECT INJECTION DIESEL ENGINE DURING THE INJECTED FUEL MASS FLOW VARIATION

PhD. Mrzljak Vedran¹, PhD Student Eng. Poljak Igor², Student Žarković Božica¹

¹Faculty of Engineering, University of Rijeka, Vukovarska 58, 51000 Rijeka, Croatia,

²Department of maritime sciences, University of Zadar, Mihovila Pavlinovica 1, 23000 Zadar, Croatia

E-mail: vedran.mrzljak@riteh.hr, ipoljak2@unizd.hr, bozica.zarkovic@gmail.com

Abstract: A change in essential operating parameters of a high speed direct injection turbocharged diesel engine MAN D0826 LOH15 during the injected fuel mass flow variation was presented. Based on two measurement sets, performed with standard diesel fuel, several operating parameters were calculated: engine torque, effective power, excess air ratio, specific effective fuel consumption and heat released per engine process. All of the calculated parameters are presented for a wide engine operating range. Along with calculated, several important parameters were measured, in addition to those presented in measurement sets. Additional measured parameters were lubrication oil temperature and exhaust gas temperature before and after the turbocharger turbine. Those calculated and measured parameters allow deep insight not just into the engine process, but also in the process of turbocharging, which is very important in the analyzed diesel engine operation.

Keywords: DIESEL ENGINE, TURBOCHARGER, FUEL MASS FLOW VARIATION, EXPERIMENTAL ANALYSIS

1. Introduction

From the invention of an internal combustion engine, experimental measurements are the basis for their operating parameters analysis, [1] and [2]. Along with internal combustion engine measurements, numerical simulations have been developed to make easier, faster and cheaper investigations of engine operating parameters.

Today, several types of diesel engine numerical models were developed: 0D (zero dimensional) models [3], multizone models [4], quasi dimensional models [5] and [6], while the last and most detailed ones are CFD (Computational Fluid Dynamic) models [7]. In order to determine the accuracy and precision of each model, they must necessarily be validated in several different measuring points of the tested engine. Therefore, experimental engine measurements are inevitable, even nowadays.

To reduce diesel engine emissions and improve engine operating parameters, researchers are intensively involved in implementing combustion of different alternative fuels in existing diesel engines. Two researches of alternative fuel usage in diesel engines are [8] and [9]. A complete review of green fuels as alternative fuels for diesel engines is presented in [10] while review of performance, combustion and emission characteristics of bio-diesel fuelled diesel engines presented authors in [11].

In this paper was presented change in the operating parameters of a high speed direct injection turbocharged diesel engine during the injected fuel mass flow variation. Operating parameters analysis was based on two measurements set at different engine rotational speeds. Measurements were obtained with a standard diesel fuel D2. Analyzed parameters can be divided in two groups: calculated ones and measured ones. Calculated operating parameters were engine torque, effective power, excess air ratio, specific effective fuel consumption and heat released per engine process. Measured operating parameters were a temperature of lubrication oil and exhaust gas temperatures before and after the turbocharger turbine. The presented operating parameters allow insight into a wide operating range of the analyzed engine.

2. Investigated diesel engine specifications

The investigated diesel engine was a high speed direct injection turbocharged diesel engine MAN D0826 LOH15, designed for a truck or small ship drive. The main engine specifications and characteristics are presented in Table 1. The piston geometry is characterized by an eccentric hole in piston head which is used for the fuel injection. In order to maximize the suction and exhaust valve flow rate, the fuel injector is positioned eccentrically and hence the hole in the piston head is positioned in the same way.

Table 1. Engine specifications

Number of cylinders	6
The total operating volume	6870 cm ³
Peak effective power	160 kW
Cylinder bore	108 mm
Cylinder stroke	125 mm
Compression ratio	18
Crank radius	62.5 mm
Length of the connecting rod	187.2 mm
Nozzle diameter	0.23 mm
Number of nozzle holes	7

3. Diesel engine measurement results and measuring equipment

Engine measurement was performed in the Laboratory for Internal Combustion Engines and Electromobility, Faculty of Mechanical Engineering, University of Ljubljana, Slovenia.

Measured engine was connected to an eddy current brake Zöllner B-350AC, Fig. 1. Measurements control was secured with a control system KS ADAC/Tornado. Cylinder pressure was measured with pressure sensor AVL GH12D, placed in an extra hole in the cylinder head. The cylinder pressure signal was led to a 4-channel amplifier AVL MicroIFEM.

The piston top dead center was determined by a capacitive sensor COM Type 2653, and the crankshaft angle was measured by crank angle encoder Kistler CAM UNIT Type 2613B with an accuracy of 0.1° crank angle.

Lubrication oil temperature was measured with Greisinger GTF 401-Pt100 Immersion probe while the flue gas temperature at the turbocharger turbine inlet and outlet was measured with two Greisinger GTF 900 Immersion probes.

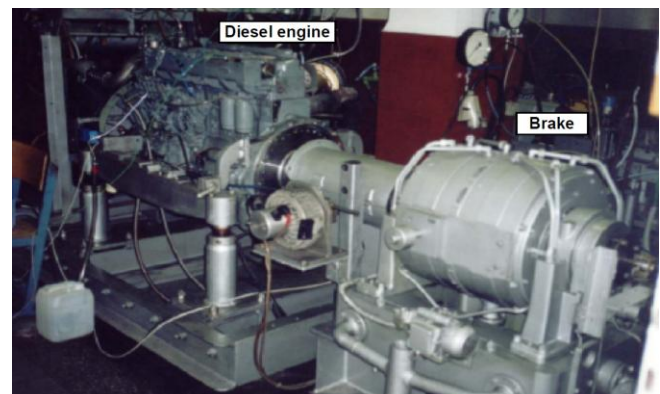


Fig. 1. Diesel engine MAN D0826 LOH15 connected to eddy current brake during the measurements

Several measurement sets were carried out and for analysis in this paper are selected two measurement sets presented in Table 2 and Table 3. Each measurement set has almost constant engine rotational speed (1500 rpm and 2400 rpm), but in each measurement set fuel and air mass flow constantly increases from operating point 1 to 4. Air mass flow must have the same trend as fuel mass flow in order to obtain complete combustion.

Table 2. Obtained measurement results - Set 1

Measurement No.	Fuel mass flow (kg/h)	Air mass flow (kg/s)	Rotational speed (rpm)	Brake reaction force (N)	BMEP* (bar)
1	9.198	0.10076	1498	292.2	5.10
2	13.447	0.11192	1502	449.7	7.86
3	18.040	0.12672	1502	594.6	10.39
4	22.453	0.14146	1501	735.0	12.84

* BMEP = Brake Medium Effective Pressure

From the measurement Set 2, Table 3, is visible that at the higher engine rotational speed (2400 rpm) injected fuel mass flow increases in comparison with measurement Set 1 (Table 2), along with simultaneous increase in air mass flow.

Table 3. Obtained measurement results - Set 2

Measurement No.	Fuel mass flow (kg/h)	Air mass flow (kg/s)	Rotational speed (rpm)	Brake reaction force (N)	BMEP* (bar)
1	14.774	0.19158	2401	234.4	4.09
2	21.815	0.22495	2402	391.1	6.83
3	28.842	0.26069	2399	525.4	9.18
4	35.364	0.29387	2399	638.4	11.15

* BMEP = Brake Medium Effective Pressure

4. Equations for calculating engine operating parameters

In each operating point engine torque was calculated according to the equation:

$$M = F \cdot R \quad (1)$$

where M (Nm) is torque, F (N) is brake reaction force and R (m) is the brake prong length on which the reaction force is measured. For eddy current brake Zöllner B-350AC, brake prong length amounts $R = 0.955$ m.

Engine effective power was calculated by using an equation:

$$P_{ef} = \frac{M \cdot 2 \cdot \pi \cdot n}{60 \cdot 1000} \quad (2)$$

where P_{ef} (kW) is effective power and n (rpm) is engine rotational speed.

Excess air ratio was calculated according to the equation:

$$\lambda = \frac{\dot{m}_a \cdot 3600}{\dot{m}_f \cdot L_{st}} \quad (3)$$

where λ (-) is excess air ratio, \dot{m}_a (kg/s) is an air mass flow, \dot{m}_f (kg/h) is the fuel mass flow and L_{st} (-) is a stoichiometric air mass, which is dependable on used fuel properties. During measurements is used standard diesel fuel D2, which lower heating value (H_d) amounts $H_d = 42700$ kJ/kg and stoichiometric air mass amounts $L_{st} = 14.7$.

Specific effective fuel consumption was calculated by using an equation:

$$b_{ef} = \frac{\dot{m}_f \cdot 1000}{P_{ef}} \quad (4)$$

where b_{ef} (g/kWh) is specific effective fuel consumption.

The heat released per process is obtained with an equation:

$$Q_{pp} = \frac{\dot{m}_f \cdot H_d}{n \cdot 60} \quad (5)$$

where Q_{pp} (kJ/proc.) is heat released per process.

5. Change in calculated and measured engine operating parameters with discussion

During the lower engine rotational speed (Set 1), an increase in engine torque is much sharper than for the higher engine rotational speed (Set 2), Fig. 2. For the engine rotational speed of 1500 rpm, maximum obtained torque was 701.93 Nm, while at a rotational speed of 2400 rpm maximum torque was 609.67 Nm. The change of engine torque, in each observed measurement set is almost linear (engine torque linearly increases with the increase in fuel mass flow). For the same fuel mass flow, significantly higher engine torque is obtained at lower engine rotational speed.

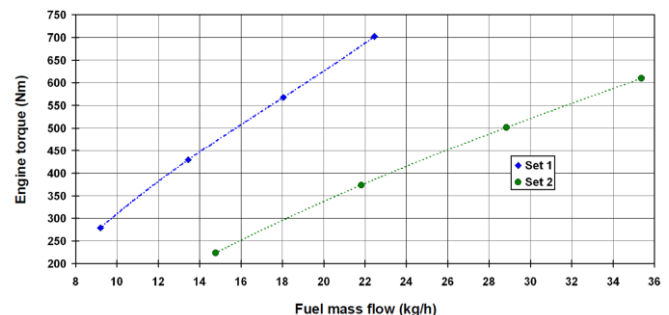


Fig. 2. Change in engine torque for each measurement set

For each engine rotational speed, effective power has the same trend - it increases during the increase in engine fuel mass flow. The maximum effective power in measurement Set 1 is 110.3 kW, while in measurement Set 2 maximum effective power amounts 153.2 kW, Fig. 3. For the same fuel mass flow, the higher effective power is obtained at lower engine rotational speed. From that fact can be concluded that for the tested engine during the same fuel mass flow, higher torque at 1500 rpm has a greater impact on engine effective power increase than the increase in rotational speed from 1500 rpm to 2400 rpm.

Gasoline engines operate strictly with air excess ratio equal to 1 (because of the three-way catalyst) while diesel engines operate with excess air ratio bigger than 1. For the analyzed engine, excess air ratio in each measurement set decreases during the increase in fuel mass flow, according to equation (3). In measurement Set 1 (1500 rpm) excess air ratio decreases from 2.68 at the lowest fuel mass flow to the 1.54 at the highest fuel mass flow, Fig. 4. In measurement Set 2 (2400 rpm) excess air ratio has significantly higher values than in measurement Set 1. In Set 2 excess air ratio

decreases from 3.18 at the lowest fuel mass flow to the 2.04 at the highest fuel mass flow. At the higher engine rotational speed, for the same fuel mass flow, the engine consumes much bigger air mass flow.

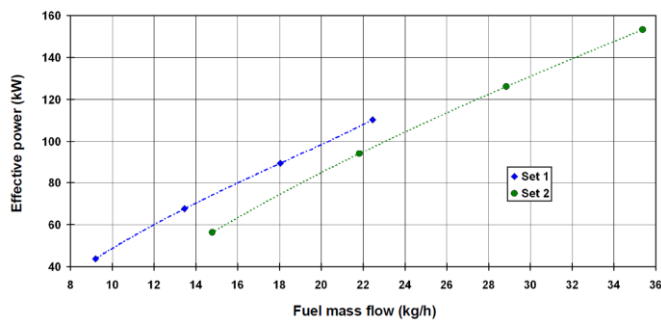


Fig. 3. Change in engine effective power for each measurement set

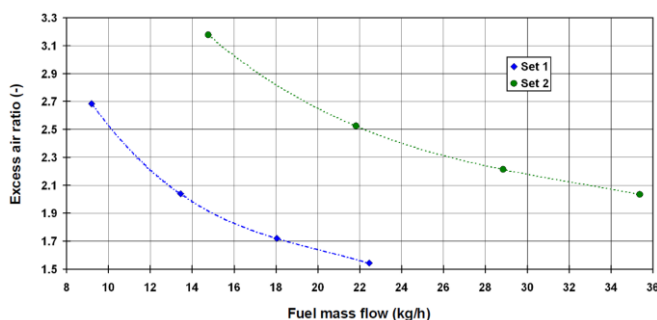


Fig. 4. Engine excess air ratio change for each measurement set

Specific effective fuel consumption, for engine measurement Set 1 and Set 2 is presented in Fig. 5. For both engine measurement sets, specific effective fuel consumption, calculated by using equation (4), firstly decreases after which follows the slight increase during the increase in fuel mass flow.

In measurement Set 1 (1500 rpm) specific effective fuel consumption amounts 210.12 g/kWh at the lowest fuel mass flow and 203.57 g/kWh at the highest fuel mass flow. The lowest value of specific effective fuel consumption in measurement Set 1 amounts 199.04 g/kWh for fuel mass flow of 13.447 kg/h.

In measurement Set 2 (2400 rpm) specific effective fuel consumption amounts 262.57 g/kWh at the lowest fuel mass flow and 230.85 g/kWh at the highest fuel mass flow. The lowest value of specific effective fuel consumption in measurement Set 2 amounts 228.82 g/kWh for fuel mass flow of 28.842 kg/h.

From Fig. 5 can be seen that at the higher engine rotational speed, specific effective fuel consumption has much higher values in comparison with the lower rotational speed.

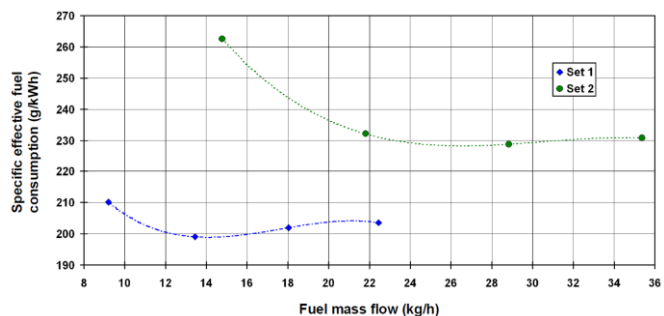


Fig. 5. Specific effective fuel consumption change for each engine measurement set

The heat released per engine process for both analyzed engine measurement sets is presented in Fig. 6. For the same fuel mass flow, heat released per engine process is much higher in Set 1 (1500 rpm) in comparison with Set 2 (2400 rpm).

In measurement Set 1 heat released per engine process amounts 4.37 kJ/proc. at the lowest fuel mass flow and 10.65 kJ/proc. at the highest fuel mass flow while in measurement Set 2 heat released per engine process amounts 4.38 kJ/proc. at the lowest fuel mass flow and 10.49 kJ/proc. at the highest fuel mass flow.

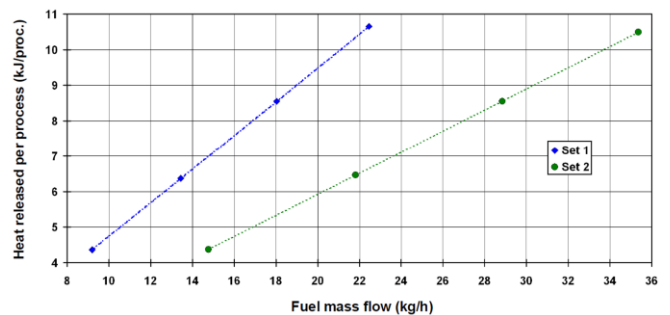


Fig. 6. The heat released per engine process change for each measurement set

A temperature change of engine lubrication oil is presented in Fig. 7 for each observed measurement set. Engine lubrication oil temperature change has the same trend in each measurement set, temperature increases during the increase in fuel mass flow. However, the curves which described oil temperature changes are not of the same type in each measurement set.

In measurement Set 1 engine lubrication oil temperature increases from 96.33 °C at the lowest fuel mass flow until 105.42 °C at the highest fuel mass flow. In measurement Set 2 engine lubrication oil temperature increases from 103.14 °C at the lowest fuel mass flow until 111.45 °C at the highest fuel mass flow.

Lubrication oil temperature is not an essential engine operating parameter, but it is important to measure it in order to maintain lubrication oil temperature within the range recommended by the producer.

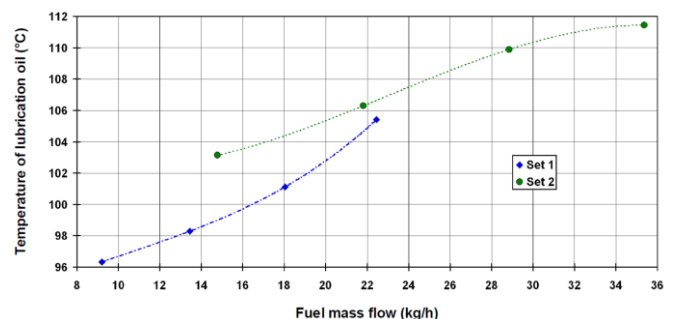


Fig. 7. Engine lubrication oil temperature change for each measurement set

Exhaust gas temperature has the highest value before the engine turbocharger turbine. It is important to measure exhaust gas temperature before and after turbine in order to calculate turbine power which is transferred directly to air blower. On that way can also be calculated air pressure after blower and compared with measurement results.

At each measurement set, exhaust gas temperature before the turbine increases during the increase in fuel mass flow, Fig. 8. In measurement Set 1 exhaust gas temperature before the turbine increases from 344.39 °C to 623.54 °C while in measurement Set 2 exhaust gas temperature before the turbine increases from 387.44 °C to 632.93 °C from the lowest to the highest fuel mass flow in each measurement set.

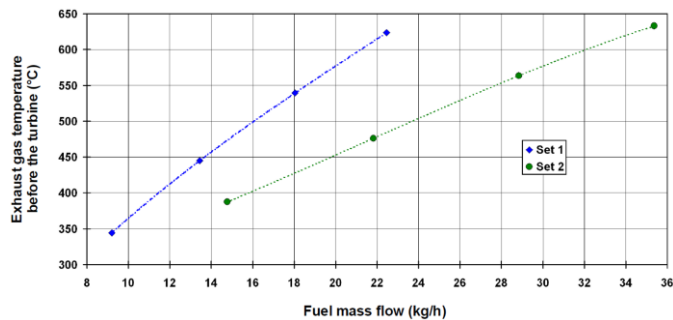


Fig. 8. The change of exhaust gas temperature before the turbine for each measurement set

Exhaust gas temperature after the turbine has the same trend as exhaust gas temperature before the turbine, Fig. 9, it increases during the increase in fuel mass flow for each measurement set. The same trend of temperatures before and after the turbine provides information about the satisfactory operation regime of turbocharger turbine, without its detail analysis.

In measurement Set 1 exhaust gas temperature after the turbine increases from 307.67 °C to 543.6 °C while in measurement Set 2 exhaust gas temperature after the turbine increases from 317.52 °C to 486.79 °C from the lowest to the highest fuel mass flow in each measurement set.

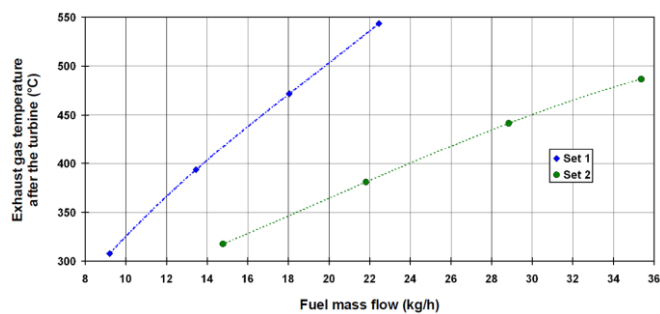


Fig. 9. The change of exhaust gas temperature after the turbine for each measurement set

6. Conclusions

In this paper is presented a change in operating parameters for a high speed direct injection turbocharged diesel engine MAN D0826 LOH15 during the injected fuel mass flow variation.

Based on a two measurement sets at different engine rotational speed (1500 rpm and 2400 rpm) is presented change of different engine operating parameters. Calculated engine operating parameters, based on measurement results, were engine torque, effective power, excess air ratio, specific effective fuel consumption and heat released per engine process.

Measured temperature of lubrication oil increases during the increase in engine fuel mass flow and it is important to maintain the oil temperature within the range recommended by the producer. Measured exhaust gas temperature change before and after the turbocharger turbine are the important elements in the analysis of turbocharging process and its efficiency.

Engine analysis was performed with standard diesel fuel. In future research will be interesting to compare the same operating parameters when engine uses alternative fuels or its blends with standard diesel fuel. This thought will be the guiding idea in future investigation of this engine.

7. Acknowledgment

The authors express their thankful regards to the whole team at the Laboratory for Internal Combustion Engines and Electromobility (LICEM), at the Faculty of Mechanical Engineering, University of Ljubljana, Slovenia. This work was supported by the University of Rijeka (contract no. 13.09.1.1.05).

8. References

- [1] Rakopoulos, C. D., Giakoumis, E. G.: *Diesel Engine Transient Operation - Principles of Operation and Simulation Analysis*, Springer-Verlag London, 2009. (doi:10.1007/978-1-84882-375-4)
- [2] Park, S., Kim, Y., Woo, S., Lee, K.: *Optimization and calibration strategy using design of experiment for a diesel engine*, Applied Thermal Engineering, 123, p. 917–928, 2017. (doi:10.1016/j.applthermaleng.2017.05.171)
- [3] Medica, V.: *Simulation of turbocharged diesel engine driving electrical generator under dynamic working conditions*, Doctoral Thesis, Rijeka, University of Rijeka, 1988.
- [4] Škifić, N.: *Influence analysis of engine equipment parameters on diesel engine characteristics*, Doctoral Thesis, Rijeka, University of Rijeka, 2003.
- [5] Mrzljak, V., Medica, V., Bukovac, O.: *Volume agglomeration process in quasi-dimensional direct injection diesel engine numerical model*, Energy, 115, p. 658–667, 2016. (doi:10.1016/j.energy.2016.09.055)
- [6] Mrzljak, V., Medica, V., Bukovac, O.: *Simulation of a Two-Stroke Slow Speed Diesel Engine Using a Quasi-Dimensional Model*, Transactions of Famena, 2, p. 35–44, 2016. (doi:10.21278/TOF.40203)
- [7] Jafari, M., Parhizkar, M.J., Amani, E., Naderan, H.: *Inclusion of entropy generation minimization in multi-objective CFD optimization of diesel engines*, Energy, 114, p. 526–541, 2016. (doi:10.1016/j.energy.2016.08.026)
- [8] Jamrozik, A.: *The effect of the alcohol content in the fuel mixture on the performance and emissions of a direct injection diesel engine fueled with diesel-methanol and diesel-ethanol blends*, Energy Conversion and Management, 148, p. 461–476, 2017. (doi:10.1016/j.enconman.2017.06.030)
- [9] Hoseini, S.S., Najafi, G., Ghobadian, B., Rahimi, A., Yusaf, T., Mamat, R., Sidik, N.A.C., Azmi, W.H.: *Effects of biodiesel fuel obtained from Salvia Macrosiphon oil (ultrasonic-assisted) on performance and emissions of diesel engine*, Energy, 131, p. 289–296, 2017. (doi:10.1016/j.energy.2017.04.150)
- [10] Othman, M.F., Adam, A., Najafi, G., Mamat, R.: *Green fuel as alternative fuel for diesel engine: A review*, Renewable and Sustainable Energy Reviews, 80, p. 694–709, 2017. (doi:10.1016/j.rser.2017.05.140)
- [11] Tamilselvan, P., Nallusamy, N., Rajkumar, S.: *A comprehensive review on performance, combustion and emission characteristics of biodiesel fuelled diesel engines*, Renewable and Sustainable Energy Reviews, 79, p. 1134–1159, 2017. (doi:10.1016/j.rser.2017.05.176)